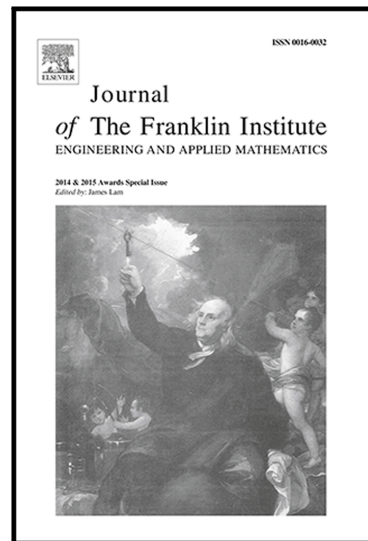


## Journal Pre-proof

Global dynamics of an epidemic model with incomplete recovery in a complex network

Aadil Lahrouz, Adel Settati, Hamza El Mahjour,  
Mustapha El Jarroudi, Mohammed El Fatini

PII: S0016-0032(20)30167-8  
DOI: <https://doi.org/10.1016/j.jfranklin.2020.03.010>  
Reference: FI 4482



To appear in: *Journal of the Franklin Institute*

Received date: 3 February 2019  
Revised date: 5 October 2019  
Accepted date: 6 March 2020

Please cite this article as: Aadil Lahrouz, Adel Settati, Hamza El Mahjour, Mustapha El Jarroudi, Mohammed El Fatini, Global dynamics of an epidemic model with incomplete recovery in a complex network, *Journal of the Franklin Institute* (2020), doi: <https://doi.org/10.1016/j.jfranklin.2020.03.010>

This is a PDF file of an article that has undergone enhancements after acceptance, such as the addition of a cover page and metadata, and formatting for readability, but it is not yet the definitive version of record. This version will undergo additional copyediting, typesetting and review before it is published in its final form, but we are providing this version to give early visibility of the article. Please note that, during the production process, errors may be discovered which could affect the content, and all legal disclaimers that apply to the journal pertain.

© 2020 Published by Elsevier Ltd on behalf of The Franklin Institute.

## Highlights

- A new epidemic model on [complex networks](#) is proposed.
- Necessary and sufficient conditions for the [stability](#) of equilibria is established.
- The influence of heterogeneous network structure on the epidemic outcome is discussed.

# Global dynamics of an epidemic model with incomplete recovery in a complex network

Aadil Lahrouz<sup>1</sup>, Adel Settati<sup>1</sup>, Hamza El Mahjour<sup>1</sup>,  
Mustapha El Jarroudi<sup>1</sup>, Mohammed El Fatini<sup>2</sup>

October 5, 2019

<sup>1</sup> Laboratory of Mathematics and Applications, Department of Mathematics, Faculty of Sciences and Techniques, B.P. 416-Tanger Principale, Tanger, Morocco.

<sup>2</sup> Ibn Tofail University, FS, Department of Mathematics, BP 133, Kénitra, Morocco.

## Abstract

In this work, we study the global dynamics of a new SIRI epidemic model with demographics, graded cure and relapse in a complex heterogeneous network. First, we analytically make out the epidemic threshold  $\mathcal{R}_0$  which strictly depends on the topology of the underlying network and the model parameters. Second, we show that  $\mathcal{R}_0$  plays the role of a necessary and sufficient condition between extinction and permanence of the disease. More specifically, by using new Lyapunov functions, we establish that the disease free-equilibrium state  $E^0$  is globally asymptotically stable when  $\mathcal{R}_0 \leq 1$ , otherwise we proved the existence and uniqueness of the endemic state  $E^*$ . Then, we show that  $E^*$  is globally asymptotically stable. Finally, we present a series of numerical simulations to confirm the correctness of the established analytical results.

**Key words:** SIRI model; Stability; Complex network.

## 1 Introduction

Communicable diseases are usually studied using compartmental models, where individuals are classified according to their infectious stage, such as susceptible, exposed, infected, or recovered. Most models are described by ordinary differential equations [3, 19, 27, 29]. While these models have shown tremendous potential, their application is limited to situations where the population is well-mixed such that the mixing of individuals is homogeneous and all hosts have identical rates of disease-causing contacts. However, it has been observed that in reality, there exist some members, called super-spreaders, who could transmit infection to many other members of the population [21]. In order to reflect the heterogeneity of contact, another approach was adopted to analyze the spread of diseases using network theory [21, 24, 33, 35, 36, 46, 55, 56]. Basically, nodes represent individuals and edges represent the contacts between them. The number of contacts is called *degree*. All individuals who have the same degree  $k$  at time  $t$  are assigned to the same compartment  $S_k(t)$ ,  $I_k(t)$  or  $R_k(t)$ . In the literature, various kinds of network's topology have been extensively described by graph theorists, we present here briefly four types : *lattice*, *random*, *small world* and *scale-free*.

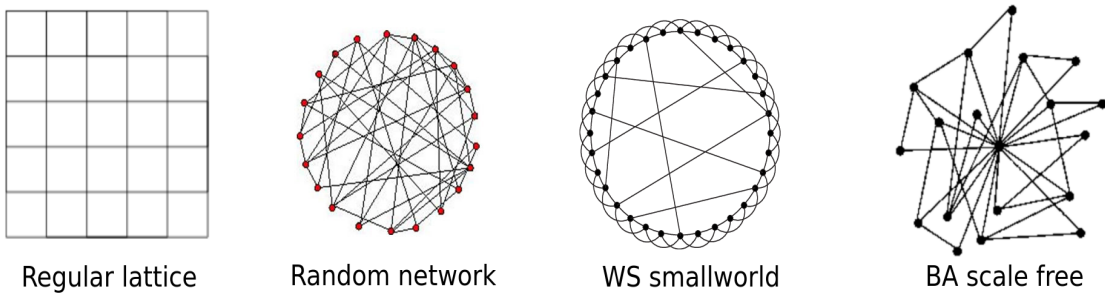


**Figure 1:** Examples of lattice, small-world, scale-free and random graphs [39].

Since the beginning of sixties of the 20<sup>th</sup> century, Erdős and Renyi worked essentially on random graphs [11, 12]. The basic idea of constructiong such graphs is to start from  $n$  nodes and then randomly create edges linking nodes with equal probability. Although, their graph model did not match real world networks [1, 7], their work was widely reused and improved to make a better representation of real networks [32]. A lattice graph, also known as a mesh graph or grid graph possesses a drawing whose embedding in a Euclidean space  $\mathbb{R}^n$  forms a regular tiling [51, 52]. These type of graphs have several applications in various domains like biology; to model the interaction between body cells, or neuroscience; to describe the complex brain network [2, 14, 15]. The structure of a lattice graph is  $k - \text{regular}$ , that is, all the nodes have the same degree [38]. If one looks at the average path length of a one dimensional regular graph, which is the number of edges between two nodes  $i$  and  $j$ , it scales as  $n$  where  $n$  is the size of the graph. However, this is not the case for random and small world graph, where it is has been proven that most vertices are connected by a short path because the average path length scales as  $\log(n)$  [4, 6, 38]. Note that the main idea of small-world graph is to make a small degree of disorder in the lattice to have short paths. But, unlike random graphs, Watts and Strogatz showed that the graph obtained is still mostly regular. For further details about small-world graphs and their properties we refer the reader to [48–50]. Although "small-world" model was a real breakthrough in the technical sense when it appeared, today it is mainly of historical interest since it is clear that it is not a good representation of real networks. Indeed, real-world networks have the scale-free feature. In fact, when the question, what is the probability  $P(k)$  that a node, in a real world network, has a degree  $k$ ? It turns out, from data collected over hundreds of real world networks, that the most accurate answer is  $P(k) = Ak^{-\eta}$ , where  $A$  is a positive constant and  $2 < \eta < 3$ . However, scientists needed an algorithm that recreates real world networks to approximate existing data. It is thanks to the groundbreaking work of Barabasi and Albert [1] that this algorithm has seen light. They analyzed data from real networks like the world wide web, and formulated an unprecedented process based on two ingredients : growth and preferential attachment. In comparison with already existing models, the simulations showed that the Barabasi-Albert model gives a better match with available data about real world networks. Later, their idea was rigorously proven by Bollobas et al. [5]. For further details, Boccaletti et al . [4] gave a major review of disparate complex networks structures and their applications. As introduced before, in epidemiology, various authors integrated complex networks as a tool to model the spread of infectious diseases. One of the pioneer works was suggested by Pastor-Satorras and Vespignani [35, 36]. They formulated the following SIS model in a scale-free

network

$$\frac{d\rho_k(t)}{dt} = -\rho_k(t) + \lambda_k(1 - \rho_k(t))\theta(t) \quad k = 1, 2, \dots, n, \quad (1)$$

where  $\rho_k(t)$  represents the relative density of infected nodes with a given degree  $k$ ,  $n$  is the maximum degree number of all nodes,  $\lambda_k > 0$  is the transmission rate,  $\theta = \frac{1}{\langle k \rangle} \sum_{i=1}^n i P(i) \rho_i$ ,

$P(i)$  is the probability that an infected node has  $i$  neighbors, and  $\langle k \rangle$  is the average connectivity of the network. The global behavior of the model (1) is studied by Wang and Dai [43] using a monotone iterative technique. Recently, there are many interesting papers that deal with the dynamics of epidemic models in network [8, 21–23, 44–47, 54]. For instance, Li et al. [21] proposed and analyzed the following network-based SIRS epidemic model with birth and death rates:

$$\begin{cases} \frac{dS_k(t)}{dt} = \mu - \mu S_k(t) - \lambda(k) S_k(t)\theta(t) + \gamma R_k(t), \\ \frac{dI_k(t)}{dt} = -(\mu + \alpha) I_k(t) + \lambda(k) S_k(t)\theta(t), \\ \frac{dR_k}{dt} = -(\mu + \gamma) R_k(t) + \alpha I_k(t), \end{cases} \quad k = 1, 2, \dots, n, \quad (2)$$

such that  $S_k(t) + I_k(t) + R_k(t) = 1$  for all  $t > 0$  and  $k = 1, 2, \dots, n$ . Here,  $n$  is the maximum degree of connectivity present in the network,  $\lambda(k) > 0$  is the degree-dependent infection rate,  $\mu$  represents the birth and death rates,  $\alpha > 0$  is the recovery rate of the infected nodes,  $\gamma > 0$  is the average loss of immunity rate,  $\theta(t)$  is the proportion of infective occupied edges over the entire network given by

$$\theta(t) = \frac{1}{\langle k \rangle} \sum_{i=1}^n \varphi(i) P(i) I_i(t),$$

such that  $\varphi(i)$  denotes the infectivity of a node with degree  $i$  where various types have been considered in the literature [24, 55, 56]. The authors in [21] found that the dynamics of the network-based SIRS model (2) is completely determined by the threshold

$$\mathcal{R}_0 = \frac{1}{(\mu + \alpha) \langle k \rangle} \sum_{k=1}^n \lambda(k) \varphi(k) P(k).$$

Indeed, if  $\mathcal{R}_0 \leq 1$  then the disease-free equilibrium is globally attractive and the disease dies out. Otherwise, the disease-free equilibrium becomes unstable and in the meantime there exists a unique endemic equilibrium state which is globally asymptotically stable. In [44], the authors investigated the global behaviour of a two-stage contact process on a complex network with heterogeneous degree distribution. In fact, they have corrected the analysis given by Masuda and Konno [26] and proved, under sufficient conditions, the global stability of disease-free and endemic equilibrium states. In [23], Liu et al. studied the transmission dynamics for Zika virus in a complex network. Using Latin Hypercube Sampling algorithm, the authors estimated  $\mathcal{R}_0$ . This method consists to consider each parameter that determines  $\mathcal{R}_0$  as a random variable in order to derive its frequency distribution. In [45], Wang and Cao proposed a network based model for waterborne diseases transmission. Using the next generation matrix method, they derived the expression of the basic reproduction number. The authors established the global stability of the disease-free equilibrium state when  $\mathcal{R}_0 < 1$ .

They also studied the global stability of the endemic equilibrium state by considering two separate cases. The first case is when immunity rate is supposed to be permanent. The second one is when indirect environment-to-human transmission is neglected and only direct human-to-human transmission rate is considered. Motivated by the previous works, in this paper we aim to study a network based epidemic model with cure, relapse and temporary immunity. Many infectious diseases need the implementation of treatments and medical care so as to stop the spread of the disease and at most cure it, especially for diseases without vaccines or that are still in development like Chikungunya or HIV-1 [34]. Also, there exist other epidemics, like tobacco, alcohol or drug consumption, where recovered individuals suffer from a relapse and become infectious again. For instance, in drug epidemic models, the path from the recovered class  $R$  back to the infective class  $I$  represents the effect of repeated drug use or the effect of heavy smokers on those who quit smoking. On one hand, literature is rich of epidemics involving the transition from  $R$ -class to  $I$ -class, these type of models are often called *SIRI* [25, 42, 53]. On the other hand, various papers study models with the transition from  $I$  to  $S$ , which are mostly known as *SIS* epidemic models [9, 10, 16]. Still, rare are the works combining both transitions. For instance, Muroya combined the relapse and cure components in one model in his paper [30]. Recently, Lahrouz et al. [20] generalized Muroya's model and proved the global stability of the disease-free and endemic equilibrium points under biologically meaningful conditions on the force of infection. In [54], the authors proposed and studied a heroin epidemic model with cure, relapse and temporary immunity on a scale-free network without demography. In this paper we aim to generalize Junyuan's paper [54] by integrating some vital dynamics with a non constant population size and with a generalized degree distribution function. We also prove the global stability of the equilibrium points under necessary and sufficient conditions. Considering a graded cure rate  $\varepsilon$  and a relapse parameter  $\sigma$ , our model can be written as follows.

$$\begin{cases} \frac{dS_k}{dt} = \mu - \mu_1 S_k - \lambda_k S_k(t)\theta(t) + \varepsilon I_k(t) + \gamma R_k(t), \\ \frac{dI_k}{dt} = -(\mu_2 + \varepsilon + \alpha)I_k(t) + \lambda_k S_k(t)\theta(t) + \sigma R_k(t), \\ \frac{dR_k}{dt} = -(\mu_3 + \gamma + \sigma)R_k(t) + \alpha I_k(t), \quad k = 1, 2, \dots, n, \end{cases} \quad (3)$$

with an initial condition that verifies

$$S_k(0), I_k(0), R_k(0) > 0, \quad \forall 1 \leq k \leq n. \quad (4)$$

And where  $\theta$  is defined as follows,

$$\theta(t) = \sum_{j=1}^n \frac{\varphi(j)P(j|k)I_j(t)}{< k >}. \quad (5)$$

We neither chose a particular probability distribution  $P$  nor specified any specific expression of the infectivity  $\varphi_j$  of a node of degree  $j$ . We want our network's topology to be as general as possible. The parameters  $\mu_1$ ,  $\mu_2$  and  $\mu_3$  represent the death rates related to the compartments  $S$ ,  $I$  and  $R$  consecutively. The recovery rate is  $\alpha$  and the immunity rate is  $\gamma$ . This paper is organized as the follows. In chapter 2 we prove the existence of equilibrium states and show the expression of the epidemic threshold  $\mathcal{R}_0$ . In chapter 3, the global stability of the disease-free equilibrium is proven when  $\mathcal{R}_0 \leq 1$ . In chapter 4, we prove that if  $\mathcal{R}_0 > 1$  then the endemic equilibrium state is globally asymptotically stable. For a lighter notation we prefer to denote  $\varphi(k) \rightarrow \varphi_k$ ,  $\lambda(k) \rightarrow \lambda_k$  and  $P(k) \rightarrow P_k$ .

## 2 Well posedness, epidemic threshold and equilibria

Let  $\mathbb{R}_+^{3n}$  be the positive cone of  $\mathbb{R}^{3n}$ , and define its subset

$$\Delta = \left\{ (x_1, y_1, z_1, \dots, x_n, y_n, z_n) \in \mathbb{R}_+^{3n}; \quad x_i + y_i + z_i < \frac{\mu}{\mu_1}, \quad \forall i = 1, \dots, n \right\}.$$

**Proposition 1.** *For every initial condition satisfying (4), the system (3) has a unique positive solution  $\overline{(S, I, R)} = (S_1, I_1, R_1, \dots, S_n, I_n, R_n)$ . Furthermore, the set  $\Delta$  is positively invariant for system (3).*

*Proof.* We should mention that the theorem of Cauchy-Lipschitz ensures the existence of a solution for system (3) on a maximal domain  $[0, T)$ . To obtain the derivative of  $\theta$  we use its definition and  $I_k$ 's equation

$$\frac{d\theta}{dt} = \underbrace{\left[ -(\mu_2 + \varepsilon + \alpha) + \sum_{< k >} \frac{\varphi_j P_j (\lambda_j S_j + R_j)}{F(t)} \right]}_{F(t)} \theta(t).$$

So,

$$\theta(t) = \theta(0) \exp \left( \int_0^t F(u) du \right) > 0. \quad (6)$$

We deduce that  $\theta(t) > 0$  for all  $t \in [0, T)$ . Take an arbitrary  $k$ , we claim that  $I_k(t) > 0$ , for all  $t \in [0, T)$ . We proceed by contradiction. Suppose that there exists a finite  $\tau_k^I$  such that

$$\tau_k^I = \inf \{0 < t < T, \quad I_k(t) = 0\}. \quad (7)$$

By the regularity of  $I_k(t)$  we must have

$$\left. \frac{dI_k}{dt} \right|_{t=\tau_k^I} \leq 0. \quad (8)$$

Using (7) and  $R_k$ 's equation we obtain :

$$\frac{dR_k}{dt} \geq -(\mu_3 + \gamma + \sigma) R_k(t), \quad \forall t \in [0, \tau_k^I].$$

By the comparison principle of ODEs we conclude that :

$$R_k(t) \geq R_k(0) \exp \left( -(\mu_3 + \gamma + \sigma)t \right) > 0, \quad \forall t \in [0, \tau_k^I]. \quad (9)$$

Furthermore, on the interval  $[0, \tau_k^I]$  we have

$$\left. \frac{dS_k}{dt} \right|_{S_k=0} = \mu + \varepsilon I_k(t) + \gamma R_k(t) > 0. \quad (10)$$

It implies immediately that

$$S_k(t) > 0, \quad \forall t \in [0, \tau_k^I]. \quad (11)$$

Using (6), (9) and (11)

$$\frac{dI_k}{dt} \Big|_{t=\tau_k^I} = \lambda_k S_k(\tau_k^I) \theta(\tau_k^I) + \sigma R_k(\tau_k^I) > 0,$$

which is a contradiction with (8). So, the solution  $\overline{(S, I, R)} = (S_1, I_1, R_1, \dots, S_n, I_n, R_n)$  remains positive along the maximal interval  $[0, T)$ . Now to prove that  $T = \infty$ , suppose that  $\overline{(S, I, R)}$  is not a global solution, then at least one of its components explodes at  $T$ . Say for a certain  $i$  we have

$$\lim_{t \rightarrow T} N_i(t) = \lim_{t \rightarrow T} [S_i(t) + I_i(t) + R_i(t)] = \infty. \quad (12)$$

On the other hand, using the assumption  $\mu_1 \leq \min(\mu_2, \mu_3)$  we have

$$\begin{aligned} \frac{dN_i(t)}{dt} &= \mu - \mu_1 S_i - \mu_2 I_i - \mu_3 R_i, \\ &\leq \mu - \mu_1 (S_i + I_i + R_i), \\ &\leq \mu - \mu_1 N_i(t). \end{aligned} \quad (13)$$

Using the comparison principle of ODEs we can deduce that

$$N_i(t) \leq \frac{\mu}{\mu_1} + (N(0) - \frac{\mu}{\mu_1}) \exp(-\mu_1 t), \quad \forall t \in [0, T). \quad (14)$$

Letting  $t \rightarrow T$  in (14) and using (12) we get

$$\infty \leq \frac{\mu}{\mu_1} + (N(0) - \frac{\mu}{\mu_1}) \exp(-\mu_1 T), \quad (15)$$

which is a contradiction. Finally, we can conclude that  $\overline{(S, I, R)}$  is a positive solution on  $[0, \infty)$ . Moreover, using (14), one can easily deduce that

$$N_i(t) = S_i(t) + I_i(t) + R_i(t) < \frac{\mu}{\mu_1}, \quad \forall i = 1, \dots, n, \quad \forall t \in [0, \infty),$$

provided starting from an initial condition in  $\Delta$ . That is,  $\Delta$  is positively invariant for the system (3).  $\square$

**Proposition 2.** For system (3), we have

1. The epidemic threshold is

$$\mathcal{R}_0 = \frac{(\mu_3 + \gamma + \sigma)S^0}{(\mu_2 + \varepsilon + \alpha)(\mu_3 + \gamma + \sigma) - \sigma\alpha} \sum_{i=1}^n \frac{\lambda_i \varphi_i P_i}{< k >}. \quad (16)$$

where  $S^0 = \frac{\mu}{\mu_1}$

2. The disease-free equilibrium  $E^0 = (E_1^0, E_2^0, \dots, E_n^0)$  exists for all parameters, where  $E_k^0 = (S^0, 0, 0)$ . The steady state  $E^0$  is asymptotically stable if  $\mathcal{R}_0 < 1$  and unstable if  $\mathcal{R}_0 > 1$ .
3. The system (3) admits an endemic equilibrium state  $E^*$  if and only if  $\mathcal{R}_0 > 1$ . Moreover,  $E^*$  is unique when it exists.

*Proof.* Obviously,  $E^0$  is an equilibrium state of system (3). Using the next-generation matrix method [41] and adapting it to fit our model, we can find the expression of the epidemic threshold  $\mathcal{R}_0$ . We will use the same notations mentionned in [41]. By following the method, we obtain the two principle matrices

$$F = \frac{S^0}{\langle k \rangle} \begin{pmatrix} \lambda_1 \varphi_1 P_1 & 0 & \dots & \lambda_1 \varphi_n P_n & 0 \\ 0 & 0 & \dots & 0 & 0 \\ \vdots & \vdots & \ddots & \vdots & \vdots \\ \lambda_n \varphi_1 P_1 & 0 & \dots & \lambda_n \varphi_n P_n & 0 \\ 0 & 0 & \dots & 0 & 0 \end{pmatrix} \quad \text{and} \quad V = \begin{pmatrix} A & 0 & \dots & 0 \\ 0 & A & \ddots & \vdots \\ \vdots & \ddots & \ddots & 0 \\ 0 & \dots & 0 & A \end{pmatrix}.$$

Where

$$A = \begin{pmatrix} \mu_2 + \varepsilon + \alpha & -\sigma \\ -\alpha & \mu_3 + \gamma + \sigma \end{pmatrix}.$$

We are interested in finding the epidemic threshold  $\mathcal{R}_0$ , that is the spectral radius of  $FV^{-1}$ . We have

$$FV^{-1} = \frac{S^0}{\frac{\langle k \rangle}{((\mu_2 + \varepsilon + \alpha)(\mu_3 + \gamma + \sigma) - \sigma\alpha)}} \begin{pmatrix} a_{11} & b_{11} & \dots & a_{1n} & b_{1n} \\ 0 & 0 & \dots & 0 & 0 \\ \vdots & \vdots & \ddots & \vdots & \vdots \\ a_{n1} & b_{n1} & \dots & a_{n2} & b_{n2} \\ 0 & 0 & \dots & 0 & 0 \end{pmatrix},$$

where  $a_{ij} = (\mu_3 + \gamma + \sigma)\lambda_i \varphi_j P_j$  and  $b_{ij} = \alpha \lambda_i \varphi_j P_j$ . Considering  $I_d$  to be the identity matrix, we can easily obtain the formula of the characteristic polynomial

$$Q(x) = \det(FV^{-1} - xI_d) = (-1)^{n+1} \left[ x - \sum_{i=1}^n \frac{(\mu_3 + \gamma + \sigma)\varphi_i \lambda_i P_i S^0}{\frac{\langle k \rangle}{((\mu_2 + \varepsilon + \alpha)(\mu_3 + \gamma + \sigma) - \sigma\alpha)}} \right] x^n \quad (17)$$

So the greatest root of  $Q$  is

$$\mathcal{R}_0 = \frac{\sum_i \lambda_i \varphi_i P_i}{\langle k \rangle} \frac{(\mu_3 + \gamma + \sigma)S^0}{((\mu_2 + \varepsilon + \alpha)(\mu_3 + \gamma + \sigma) - \sigma\alpha)}, \quad (18)$$

It is straightforward to verify that assumptions (A1) - (A5) in [41] hold. It follows from Theorem 2 in [41] that  $E^0$  is asymptotically stable if  $\mathcal{R}_0 < 1$  and unstable if  $\mathcal{R}_0 > 1$ . For a positive equilibrium state, we solve the system

$$0 = \mu - \mu_1 S_k^* - \lambda_k S_k^* \theta^* + \varepsilon I_k^* + \gamma R_k^*, \quad (19)$$

$$0 = -(\mu_2 + \varepsilon + \alpha) I_k^* + \lambda_k \theta^* S_k^* + \sigma R_k^*, \quad (20)$$

$$0 = -(\mu_3 + \gamma + \sigma) R_k^* + \alpha I_k^*. \quad (21)$$

and  $S_k^*, I_k^*, R_k^* > 0$ ,  $k = 1 \dots n$ . From (21) we get

$$R_k^* = \frac{\alpha}{\mu_3 + \gamma + \sigma} I_k^*. \quad (22)$$

Multiply (21) by  $\frac{\sigma}{\mu_3 + \gamma + \sigma}$  and add it to (20) and use (22) to get

$$S_k^* = \frac{I_k^*}{\lambda_k \theta^*} \left( \mu_2 + \varepsilon + \alpha - \frac{\sigma \alpha}{\mu_3 + \gamma + \sigma} \right), \quad (23)$$

where

$$\theta^* = \frac{\sum_j \varphi_j P_j I_j^*}{\langle k \rangle}.$$

Adding (19), (20), (21) and using (22) and (23), we obtain

$$I_k^* = \frac{\mu(\mu_3 + \gamma + \sigma) \lambda_k \theta^*}{\mu_1(\mu_2 + \varepsilon + \alpha) + (\mu_2(\mu_3 + \gamma + \sigma) + \mu_3 \alpha) \lambda_k \theta^*}. \quad (24)$$

From (24), we get

$$\begin{aligned} \theta^* &= \frac{1}{\langle k \rangle} \sum_j^n \frac{\mu(\mu_3 + \gamma + \sigma) \varphi_j P_j \lambda_j \theta^*}{\mu_1((\mu_3 + \gamma + \sigma)(\mu_2 + \varepsilon + \alpha) - \sigma \alpha) + (\mu_2(\mu_3 + \gamma + \sigma)) \lambda_j \theta^*} \\ &:= f(\theta^*). \end{aligned} \quad (25)$$

It follows from (22), (23) and (24) that to show the existence of an endemic steady state for system (3), it is sufficient to establish the existence of  $\theta^* > 0$  such that  $f(\theta^*) = \theta^*$ . Define the function

$$g(\theta) = f(\theta) - \theta.$$

We can easily see that  $g''(\theta) < 0$  on  $[0, +\infty)$ , so  $g'(\theta)$  is a decreasing function. Moreover, we have

$$g'(0) = \mathcal{R}_0 - 1 \quad \text{and} \quad \lim_{\theta \rightarrow \infty} g'(\theta) = -1. \quad (26)$$

Therefore, we have two cases :

- if  $\mathcal{R}_0 \leq 1$  then  $g'(0) \leq 0$  so  $g(\theta)$  is decreasing and vanishes only at 0. Thus, there is no positive equilibrium point for the system (3).
- If  $\mathcal{R}_0 > 1$  then,  $g'(0) > 0$ . Thereby,  $g'(\theta) = 0$  has a unique solution  $\tilde{\theta} > 0$ . Hence,  $g(\theta)$  is increasing on  $[0, \tilde{\theta}]$  and decreasing on  $[\tilde{\theta}, \infty)$ .

Since,

$$\lim_{\theta \rightarrow \infty} g(\theta) = 0 \quad \text{and} \quad \lim_{\theta \rightarrow \infty} g(\theta) = -\infty, \quad (27)$$

we conclude that  $f(\theta) = \theta$  admits a unique positive solution on  $[\tilde{\theta}, \infty)$ .  $\square$

**Remark 1.** In the homogeneous case, the classes  $S_k$ ,  $I_k$  and  $R_k$  become  $S, I$  and  $R$  and the equivalent of the term  $\lambda_k S_k(t) \theta(t)$  is  $\beta SI$ , where  $\beta$  is the usual infection rate. In this case, the authors in [20] found that the expression of  $\mathcal{R}_0$  is

$$\mathcal{R}_0 = \frac{\beta S^0}{\mu_2 + \varepsilon + \alpha - \frac{\sigma \alpha}{\mu_3 + \gamma + \sigma}},$$

which represents the average number of secondary cases produced by a single infectious individual introduced in a fully susceptible host population. Similarly, assume that a single

infectious individual of degree  $j = 1 \dots n$  is introduced in the fully susceptible complex network at time  $t = 0$ . That is

$$I_j(0) = 1, \quad I_i(0) = 0, \quad \forall i \neq j.$$

By the uniqueness of the solution of system (3), one can derive that  $I_i(t) = 0$  for all  $i \neq j$  and for all  $t > 0$ . In other words, this single infectious person can produce a new infection only by contacting susceptible individuals from compartment  $S_j$  where  $S_j \approx \frac{\mu}{\mu_1} = S^0$ . Hence, in average, one have  $\frac{1}{<k>} \lambda_j \varphi_j P_j S^0$  new infected individuals. Moreover, as in [20, 40], the total average time spent in the infectious class on multiple passes is

$$\frac{1}{\mu_2 + \varepsilon + \lambda} \sum_{k=0}^{\infty} \left( \frac{\sigma \lambda}{(\mu_2 + \varepsilon + \lambda)(\mu_3 + \gamma + \sigma)} \right)^k = \frac{1}{\mu_2 + \varepsilon + \lambda - \frac{\sigma \lambda}{\mu_3 + \gamma + \sigma}}.$$

Therefore, the mean number of new infectious cases produced by one infected person of degree  $j$  during its infectivity period is

$$\mathcal{R}_0^j \triangleq \frac{1}{<k>} \lambda_j \varphi_j P_j \frac{S^0}{\mu_2 + \varepsilon + \lambda - \frac{\sigma \lambda}{\mu_3 + \gamma + \sigma}}.$$

Thus, the total average number of new infections caused by one infectious individual is

$$\mathcal{R}_0 = \frac{1}{<k>} \sum_{j=1}^n \mathcal{R}_0^j.$$

### 3 Global stability of disease-free equilibrium state

**Theorem 3.1.** If  $\mathcal{R}_0 \leq 1$  then  $E^0$  is globally asymptotically stable.

*Proof.* Define

$$L_1(t) = \frac{1}{<k>} \sum_j \frac{\varphi_j P_j}{S^0} \int_{S^0}^{S_j(t)} (x - S^0) dx, \quad L_2(t) = \theta(t) \quad \text{and} \quad L_3(t) = \sum_j \varphi_j P_j R_j.$$

We have

$$\frac{dL_1}{dt} = \frac{1}{<k>} \sum_j \frac{\varphi_j P_j}{S^0} (S_j - S^0) \frac{dS_j}{dt}.$$

Since  $\mu = \mu_1 S^0$ , we rewrite

$$\frac{dS_j}{dt} = -\mu_1 (S_j - S^0) - \lambda_j \theta(t) (S_j - S^0) - \lambda_j S^0 \theta(t) + \varepsilon I_j(t) + \gamma R_j(t).$$

Hence

$$\begin{aligned} \frac{dL_1}{dt} &= \frac{1}{S^0 <k>} \sum_j \varphi_j P_j \left[ -(\mu_1 + \lambda_j \theta) (S_j - S^0)^2 + \varepsilon (S_j - S^0) I_j + \gamma (S_j - S^0) R_j \right] \\ &+ \frac{\theta}{<k>} \sum_j \lambda_j \varphi_j P_j S^0 - \theta \sum_j \lambda_j \varphi_j P_j S_j. \end{aligned}$$

Since for all  $j$  and  $t$  we know that  $S_j(t) \leq \frac{\mu}{\mu_1} = S^0$  and  $S_j, I_j, R_j$  are positive, we obtain

$$\frac{dL_1}{dt} \leq \theta \left( \frac{\sum_j \varphi_j \lambda_j P_j S^0}{\langle k \rangle} - \frac{\sum_j \varphi_j \lambda_j P_j S_j}{\langle k \rangle} \right) - \mu_1 \frac{\varphi_j P_j (S_j - S^0)^2}{\langle k \rangle S^0}. \quad (28)$$

We have

$$\frac{dL_2}{dt} = -(\mu_2 + \varepsilon + \alpha)\theta + \frac{\theta}{\langle k \rangle} \sum_j \lambda_j \varphi_j P_j S_j + \frac{\sigma}{\langle k \rangle} \sum_j \lambda_j \varphi_j P_j R_j. \quad (29)$$

Furthermore

$$\frac{dL_3}{dt} = -\frac{\sigma}{\langle k \rangle} \sum_j \varphi_j P_j R_j + \frac{\alpha\sigma}{\mu_3 + \gamma + \sigma} \theta. \quad (30)$$

Consider

$$L(t) = L_1(t) + L_2(t) + L_3(t),$$

of course,  $L(t)$  is definite positive function. Using (28), (29) and (30), we obtain

$$\begin{aligned} \frac{dL}{dt} &\leq -\theta \overbrace{\left( \mu_2 + \varepsilon + \alpha - \frac{\sigma\alpha}{\mu_3 + \gamma + \sigma} \right)}^{m \geq 0} \left( 1 - \frac{\sum_j \lambda_j \varphi_j P_j S^0}{\langle k \rangle \left( \mu_2 + \varepsilon + \alpha - \frac{\sigma\alpha}{\mu_3 + \gamma + \sigma} \right)} \right) \\ &\quad - \mu_1 \frac{\varphi_j P_j (S_j - S^0)^2}{\langle k \rangle S^0}. \end{aligned}$$

So,

$$\frac{dL}{dt} \leq -m\theta(1 - \mathcal{R}_0) - \mu_1 \sum_j \frac{\varphi_j P_j (S_j - S^0)^2}{\langle k \rangle S^0}. \quad (31)$$

- **Case 1 :** If  $\mathcal{R}_0 < 1$ , then  $L$  is a Lyapunov function for  $E^0$ . Thus, by Lyapunov asymptotic theorem (see Theorem 3 in [37, p.131])  $E^0$  is globally asymptotically stable.
- **Case 2 :** If  $\mathcal{R}_0 = 1$ , we point out that (31) just gives the asymptotic stability of  $E^0$ . To carry out the global stability we introduce the function

$$\tilde{L}(t) = \sum_j \frac{\varphi_j P_j}{S^0 \langle k \rangle} \int_{S^0}^{N_j(t)} (x - S^0) dx.$$

So,

$$\begin{aligned} \frac{d\tilde{L}}{dt} &= \sum_j \frac{\varphi_j P_j}{S^0 \langle k \rangle} (S_j - S^0 + I_j + R_j) (-\mu_1(S_j - S^0) - \mu_2 I_j - \mu_3 R_j) \\ &= \sum_j \frac{\varphi_j P_j}{S^0 \langle k \rangle} \left[ -\mu_1(S_j - S^0)^2 - \mu_2 I_j^2 - \mu_3 R_j^2 + (\mu_1 + \mu_2)(S^0 - S_j)I_j \right. \\ &\quad \left. + (\mu_1 + \mu_3)(S^0 - S_j)R_j - (\mu_2 + \mu_3)R_j I_j \right] \end{aligned}$$

Therefore

$$\begin{aligned} \frac{d\tilde{L}}{dt} &\leq \sum_j \frac{\varphi_j P_j}{S^0 < k >} \left[ -\mu_1(S_j - S^0)^2 - \mu_2 I_j^2 - \mu_3 R_j^2 + (\mu_1 + \mu_2)(S^0 - S_j)I_j \right. \\ &\quad \left. + (\mu_1 + \mu_3)(S^0 - S_j)R_j \right]. \end{aligned} \quad (32)$$

For  $\varepsilon_1, \varepsilon_2 > 0$ , we have the elementary inequalities:

$$(S^0 - S_j)I_j \leq \varepsilon_1 I_j^2 + \frac{1}{4\varepsilon_1} (S^0 - S_j)^2, \quad (33)$$

$$(S^0 - S_j)R_j \leq \varepsilon_2 R_j^2 + \frac{1}{4\varepsilon_2} (S^0 - S_j)^2. \quad (34)$$

Using (33) and (34) in (32) we get

$$\begin{aligned} \frac{d\tilde{L}}{dt} &\leq \sum_j \frac{\varphi_j P_j}{S^0 < k >} \left[ \left( \frac{(\mu_1 + \mu_2)}{4\varepsilon_1} + \frac{(\mu_1 + \mu_3)}{4\varepsilon_2} + \mu_1 \right) (S_j - S^0)^2 \right. \\ &\quad \left. - \left( \mu_2 - (\mu_1 + \mu_2)\varepsilon_1 \right) I_j^2 - \left( \mu_3 - (\mu_1 + \mu_3)\varepsilon_2 \right) R_j^2 \right]. \end{aligned} \quad (35)$$

Let  $A > 0$ , combining (31) and (32), the derivative of the function  $AL + \tilde{L}$  along trajectories of the system (3), is given by

$$\begin{aligned} \frac{d(AL + \tilde{L})}{dt} &\leq \sum_j \frac{\varphi_j P_j}{S^0 < k >} \left[ \left( \frac{(\mu_1 + \mu_2)}{4\varepsilon_1} + \frac{(\mu_1 + \mu_3)}{4\varepsilon_2} + \mu_1 - A\mu_1 \right) (S_j - S^0)^2 \right. \\ &\quad \left. - \left( \mu_2 - (\mu_1 + \mu_2)\varepsilon_1 \right) I_j^2 - \left( \mu_3 - (\mu_1 + \mu_3)\varepsilon_2 \right) R_j^2 \right]. \end{aligned} \quad (36)$$

Finally, by choosing  $\varepsilon_1, \varepsilon_2$  so small and  $A$  sufficiently large, we can ensure that the coefficients of  $(S^0 - S_j)^2$ ,  $I_j^2$  and  $R_j^2$  are negative. That is,  $AL + \tilde{L}$  is a Lyapunov function and  $E^0$  is globally asymptotically stable.

□

## 4 Global stability of the endemic state

**Theorem 4.1.** *If  $\mathcal{R}_0 > 1$  then  $E^*$  is globally asymptotically stable.*

*Proof.* From  $I_k$ -equations we deduce that

$$\frac{d\theta}{dt} = -(\mu_2 + \varepsilon + \alpha)\theta + \frac{1}{< k >} \sum_j \lambda_j \varphi_j P_j S_j \theta + \sigma \Gamma. \quad (37)$$

Where

$$\Gamma(t) = \frac{1}{< k >} \sum_j \varphi_j P_j R_j(t). \quad (38)$$

Set

$$\Gamma^* = \frac{1}{\langle k \rangle} \sum_j \varphi_j P_j R_j^*. \quad (39)$$

Then using the equations (19),(20) and (21) we obtain

$$\frac{d\Gamma}{dt} = -(\mu_3 + \gamma + \sigma)\Gamma + \alpha\theta = \alpha\left(\frac{\theta}{\Gamma} - \frac{\theta^*}{\Gamma^*}\right). \quad (40)$$

Now, we define

$$\Lambda_1(t) = \int_{\theta^*}^{\theta(t)} \left( \frac{x - \theta^*}{x} \right) dx + \frac{\sigma\Gamma^*}{\alpha\theta^*} \int_{\Gamma^*}^{\Gamma(t)} \left( \frac{x - \Gamma^*}{x} \right) dx. \quad (41)$$

So, by (37) and (40), we get

$$\begin{aligned} \frac{d\Lambda_1(t)}{dt} &= \frac{1}{\langle k \rangle} \sum_j \lambda_j \varphi_j P_j (S_j - S_j^*)(\theta - \theta^*) \\ &\quad + \underbrace{\sigma\Gamma^* \left[ \left( \frac{\theta^*\Gamma}{\theta\Gamma^*} - 1 \right) \left( \frac{\theta}{\theta^*} - 1 \right) + \left( \frac{\theta\Gamma^*}{\theta^*\Gamma} - 1 \right) \left( \frac{\Gamma}{\Gamma^*} - 1 \right) \right]}_{\leq 0} \\ \frac{d\Lambda_1(t)}{dt} &\leq \frac{1}{\langle k \rangle} \sum_j \lambda_j \varphi_j P_j (S_j - S_j^*)(\theta - \theta^*). \end{aligned} \quad (42)$$

On the other hand, using again  $S_j$ -equation at the state  $E^*$ , we obtain

$$\begin{aligned} \frac{dS_j}{dt} &= -\mu_1(S_j - S_j^*) - \lambda_j\theta(S_j - S_j^*) - \lambda_j S_j^*(\theta - \theta^*) \\ &\quad + \varepsilon(I_j - I_j^*) + \gamma(R_j - R_j^*). \end{aligned}$$

So, if we define

$$\Lambda_2(t) = \frac{1}{\langle k \rangle} \sum_j \frac{\varphi_j P(j)}{S_j^*} \int_{S_j^*}^{S_j(t)} x - S_j^* dx,$$

we obtain

$$\begin{aligned} \frac{d\Lambda_2(t)}{dt} &= -\frac{1}{\langle k \rangle} \sum_j \frac{\varphi_j P(j)}{S_j^*} (\mu_1 + \lambda_j\theta)(S_j - S_j^*)^2 \\ &\leq -\frac{1}{\langle k \rangle} \sum_j \lambda_j \varphi_j P_j (S_j - S_j^*)(\theta - \theta^*) \\ &\quad + \frac{\varepsilon}{\langle k \rangle} \sum_j \frac{\varphi_j P_j}{S_j^*} (S_j - S_j^*)(I_j - i_j^*) \\ &\quad + \frac{\gamma}{\langle k \rangle} \sum_j \frac{\varphi_j P_j}{S_j^*} (S_j - S_j^*)(R_j - R_j^*). \end{aligned} \quad (43)$$

Put  $N_j = S_j + I_j + R_j$  and  $N_j^* = S_j^* + I_j^* + R_j^*$ . We have

$$\begin{aligned} \frac{dN_j}{dt} &= \mu - \mu_1 S_j - \mu_2 I_j - \mu_3 R_j \\ &= \mu - \mu_1 N_j - (\mu_2 - \mu_1) I_j - (\mu_3 - \mu_1) R_j. \end{aligned}$$

We also have

$$\begin{aligned} \frac{d}{dt} \left( N_j + \frac{\mu_2 - \mu_1}{\alpha} R_j \right) &= \mu - \mu_1 N_j - \underbrace{\left( \mu_3 - \mu_1 + \frac{(\mu_2 - \mu_1)(\mu_3 + \gamma + \sigma)}{\alpha} \right)}_{\kappa} R_j \\ &= -\mu_1(N_j - N_j^*) - \kappa(R_j - R_j^*). \end{aligned} \quad (44)$$

Furthermore,

$$\begin{aligned} \frac{dR_j}{dt} &= -(\mu_3 + \gamma + \sigma)R_j + \alpha I_j \\ &= -(\mu_3 + \gamma + \sigma)(R_j - R_j^*) + \alpha(I_j - I_j^*). \end{aligned} \quad (45)$$

Define

$$\Lambda_3(t) = \frac{\gamma}{\langle k \rangle \left( \kappa + \frac{\mu_1(\mu_2 - \mu_1)}{\alpha} \right)} \sum_j \frac{\varphi_j P_j}{S_j^*} \Lambda_{3j}(t), \quad (46)$$

where

$$\Lambda_{3j} = \int_{N_j^* + \frac{\mu_2 - \mu_1}{\alpha}}^{N_j(t) + \frac{\mu_2 - \mu_1}{\alpha} R_j} \left( x - N_j^* - \frac{\mu_2 - \mu_1}{\alpha} R_j^* \right) dx + \frac{\kappa + \frac{\mu_1(\mu_2 - \mu_1)}{\alpha}}{\alpha} \int_{R_j^*}^{R_j(t)} (x - R_j^*) dx. \quad (47)$$

Using (44) and (45), we obtain

$$\begin{aligned} \frac{d\Lambda_{3j}}{dt} &= -\mu_1(N_j - N_j^*)^2 - \frac{\kappa(\mu_2 - \mu_1)}{\alpha}(R_j - R_j^*)^2 - \left( \kappa + \frac{\mu_1(\mu_2 - \mu_1)}{\alpha} \right) (N_j - N_j^*)(R_j - R_j^*) \\ &\quad - \frac{(\kappa + \frac{\mu_1(\mu_2 - \mu_1)}{\alpha})(\mu_3 + \sigma + \gamma)}{\alpha} (R_j - R_j^*)^2 + \left( \kappa + \frac{\mu_1(\mu_2 - \mu_1)}{\alpha} \right) (R_j - R_j^*)(I_j - I_j^*) \\ &\leq -\left( \kappa + \frac{\mu_1(\mu_2 - \mu_1)}{\alpha} \right) \underbrace{(N_j - N_j^* - (I_j - I_j^*))}_{(S_j - S_j^*) + (R_j - R_j^*)} (R_j - R_j^*) \\ &\leq -\left( \kappa + \frac{\mu_1(\mu_2 - \mu_1)}{\alpha} \right) (S_j - S_j^*)(R_j - R_j^*). \end{aligned}$$

Therefore,

$$\frac{d\Lambda_3(t)}{dt} \leq -\frac{\gamma}{\langle k \rangle} \sum_j \frac{\varphi_j P_j}{S_j^*} (S_j - S_j^*)(R_j - R_j^*). \quad (48)$$

We have

$$\begin{aligned} \frac{d}{dt} (S_j + I_j) &= \mu - \mu_1 S_j - (\mu_2 + \alpha) I_j + (\gamma + \sigma) R_j \\ &= -\mu_1(S_j - S_j^*) - (\mu_2 + \alpha)(I_j - I_j^*) + (\gamma + \sigma)(R_j - R_j^*), \end{aligned}$$

and

$$\frac{dN_j}{dt} = -\mu_1(S_j - S_j^*) - \mu_2(I_j - I_j^*) - \mu_3(R_j - R_j^*).$$

We define

$$\Lambda_{4,1,j}(t) = \int_{S_j^* + I_j^*}^{S_j(t) + I_j(t)} (x - S_j^* - I_j^*) dx, \quad \Lambda_{4,2,j}(t) = \int_{N_j^*}^{N_j(t)} (x - N_j^*) dx, \quad \Lambda_{4,3,j} = \int_{R_j^*}^{R_j} (x - R_j^*) dx.$$

We take consecutively the derivatives of the above functions

$$\begin{aligned} \frac{d\Lambda_{4,1,j}}{dt} &= -\mu_1(S_j - S_j^*)^2 - (\mu_2 + \alpha)(I_j - I_j^*)^2 - (\mu_1 + \mu_2 + \alpha)(S_j - S_j^*)(I_j - I_j^*) - (\mu_2 + \alpha)(I_j - I_j^*)^2 \\ &\quad + (\gamma + \sigma)(S_j - S_j^*)(R_j - R_j^*) + (\gamma + \sigma)(R_j - R_j^*)(I_j - I_j^*) \\ &\leq -(\mu_1 + \mu_2 + \alpha)(S_j - S_j^*)(I_j - I_j^*) + (\gamma + \sigma)(S_j - S_j^*)(R_j - R_j^*) \\ &\quad + (\gamma + \sigma)(R_j - R_j^*)(I_j - I_j^*). \end{aligned} \quad (49)$$

$$\begin{aligned} \frac{d\Lambda_{4,2,j}}{dt} &= -\mu_1(S_j - S_j^*)^2 - \mu_2(I_j - I_j^*)^2 - \mu_3(R_j - R_j^*)^2 \\ &\quad - (\mu_1 + \mu_2)(S_j - S_j^*)(I_j - I_j^*) - (\mu_1 + \mu_3)(S_j - S_j^*)(R_j - R_j^*) \\ &\quad - (\mu_2 + \mu_3)(R_j - R_j^*)(I_j - I_j^*). \end{aligned} \quad (50)$$

$$\begin{aligned} \frac{d\Lambda_{4,3,j}}{dt} &= -(\mu_3 + \gamma + \sigma)(R_j - R_j^*)^2 + \alpha(R_j - R_j^*)(I_j - I_j^*) \\ &\leq \alpha(R_j - R_j^*)(I_j - I_j^*). \end{aligned} \quad (51)$$

Define

$$\Lambda_{4,j} = \frac{\mu_1 + \mu_3}{\sigma + \gamma} \Lambda_{4,1,j} + \Lambda_{4,2,j} + \frac{\mu_2 - \mu_1}{\alpha} \Lambda_{4,3,j}. \quad (52)$$

Combine (49), (50) and (51) to get

$$\begin{aligned} \frac{d\Lambda_{4,j}}{dt} &\leq -\mu_1(S_j - S_j^*)^2 - \mu_2(I_j - I_j^*)^2 - \mu_3(R_j - R_j^*)^2 \\ &\quad - \underbrace{\left( \frac{(\mu_1 + \mu_3)(\mu_1 + \mu_2 + \alpha)}{\alpha + \sigma} + \mu_1 + \mu_2 \right)}_{\nu} (S_j - S_j^*)(I_j - I_j^*). \end{aligned} \quad (53)$$

Now we define the function

$$\Lambda_4(t) = \frac{\varepsilon}{\nu < k >} \sum_j \frac{\varphi_j P_j}{S_j^*} \Lambda_{4,j},$$

From (53), one can deduce that

$$\begin{aligned} \frac{d\Lambda_4(t)}{dt} &\leq -\frac{\mu_1}{\nu < k >} \sum_j \frac{\varphi_j P_j}{S_j^*} (S_j - S_j^*)^2 - \frac{\mu_2}{\nu < k >} \sum_j \frac{\varphi_j P_j}{S_j^*} (I_j - I_j^*)^2 \\ &\quad - \frac{\mu_3}{\nu < k >} \sum_j \frac{\varphi_j P_j}{S_j^*} (R_j - R_j^*)^2 - \frac{\varepsilon}{< k >} \sum_j \frac{\varphi_j P_j}{S_j^*} (S_j - S_j^*)(I_j - I_j^*). \end{aligned} \quad (54)$$

Finally, we define the positive definite function

$$\Lambda(t) = \sum_{i=1}^4 \Lambda_i(t). \quad (55)$$

By combining (42), (43), (48) and (54), we conclude that

$$\begin{aligned} \frac{d\Lambda}{dt} &\leq -\frac{\mu_1}{\nu < k >} \sum_j \frac{\varphi_j P_j}{S_j^*} (S_j - S_j^*)^2 - \frac{\mu_2}{\nu < k >} \sum_j \frac{\varphi_j P_j}{S_j^*} (I_j - I_j^*)^2 \\ &\quad - \frac{\mu_3}{\nu < k >} \sum_j \frac{\varphi_j P_j}{S_j^*} (R_j - R_j^*)^2 \end{aligned}$$

Thus,  $\frac{d\Lambda}{dt}$  is negative definite along the trajectory of any solution of the system (3). Consequently,  $E^*$  is globally asymptotically stable.  $\square$

## 5 Discussion and numerical results

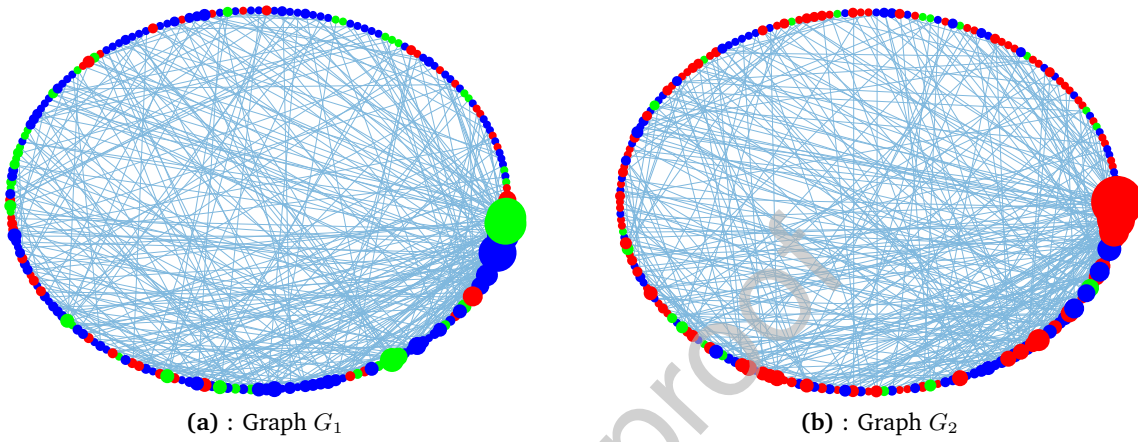


**Figure 2:** The nodes in blue represent susceptibles, infectives are in red and recovereds in green. The greater the diameter of a node is, the higher is its number of links.

In this section, we perform some numerical simulations by the Matlab software to illustrate the asymptotic stability results established in the above analysis. In Fig. 2, we simulate two initial conditions that respect a Barabasi-Albert topology. Indeed, following the principles of growth and preferential attachment, the created algorithm begins with  $m_0 = 2$  nodes, and adds a node with  $m = 2$  links at each step, until it arrives to a total size of population equal to 200. Whenever a node is added, it chooses how to connect to previous nodes according to their degree. Thus, older nodes with higher degree are most likely to get linked to the new node. Once the construction of the graph is complete, the algorithm randomly assigns nodes to a susceptible, infective or recovered class. For example, in the graph  $G_1$  (see Table 1 and Figure 2 (a)), 20% of the population is infected whereas in the graph  $G_2$  (see Table 1 and Figure 2 (b)), there are 50% of infective nodes. To obtain an approximate solution of the ordinary differential system (3), we use Euler's scheme with a time step equal to  $10^{-2}$ . Along these simulations, we use the parameters in Table 2 and we choose  $\varphi(k) = k$  and  $\lambda_k = \beta k$ , where  $\beta$  is a homogeneous infection rate. Therefore, the expression of  $\mathcal{R}_0$  becomes

$$\mathcal{R}_0 = \frac{\beta(\mu_3 + \gamma + \sigma)S^0}{(\mu_2 + \varepsilon + \alpha)(\mu_3 + \gamma + \sigma) - \sigma\alpha} \sum_{i=1}^n \frac{i^2 P_i}{<k>}.$$

It is known, by the preferential attachment principle during the construction of the graph that the probabilities are given by the following expression

$$P_i = \frac{\text{Number of nodes with degree } i}{\text{Total number of degrees}}.$$

In the analytical part, we carried out the long time behaviour of individuals (nodes) who share the same compartment and degree  $k$ , so the results shown below simulate an infection

during a period of 500 days. However, the maximum number of connections is high in both simulations. Therefore, if we represent the time series of all  $S_k$ ,  $I_k$  and  $R_k$ , it will be difficult to distinguish between them. So, Fig. 3 and Fig. 4, show the time series corresponding to some chosen degrees  $k$ . By numerical computations, one can verify that the parameters chosen for Fig. 3 satisfy  $\mathcal{R}_0 \simeq 0,416 < 1$  (see Table 2). It is clear from Fig. 3 that the disease dies out from the host population because the number of infective nodes with a positive degree converges to 0. Also the susceptibles converge to  $\frac{\mu}{\mu_1} = 10$  and the recovereds to 0. Hence, for  $\mathcal{R}_0 \leq 1$ , the convergence to the disease-free equilibrium state is numerically verified. It is also interesting to point out that we started from different initial conditions with higher percentage of infective individuals in the graph  $G_2$ . However, the outcome is the same after a certain period of time and it is totally dictated by the parameters used in the dynamical system. It is the global behaviour that takes over. Beside, the case when  $\mathcal{R}_0 \simeq 4,16 > 1$  is illustrated in Figure 4 with the parameters listed in Table 2. We see that the disease persists which is clearly indicated by the convergence of quantities  $S_k$ ,  $I_k$  and  $R_k$  to a positive equilibrium point. Remark that from the presented numerical simulations, the only information we have about the graph is the number of nodes with the same degree  $k$ . This is insufficient to build the final structure of the graph associated to the host population. This is because we do not know how the nodes are related to one another. In [18], the authors gave a pseudo-algorithm based on Havel-Hakimi and Erdős-Gallai theorems to use a degree based algorithm construction to construct an appropriate graph. In future works, we might think about how to shape this relationship between the network topology and the dynamical system. We also observe that the topology of the network does not affect the stability of the equilibrium points. Furthermore, note that in a scale-free network graph, the quantity

$$\langle k^2 \rangle = \sum_{i=1}^n i^2 P_i, \quad (56)$$

which describes the fluctuations of the connectivity distribution, diverges when the size of the graph  $n$  goes to  $\infty$ .

	Susceptibles	Infectives	Recovered
Graph $G_1$	120	40	40
Graph $G_2$	80	100	20

**Table 1:** Number of susceptible, infectious and recovered individuals in the graphs  $G_1$  and  $G_2$  which represent the two initial values used in numerical simulations.

	$\mu$	$\mu_1$	$\mu_2$	$\mu_3$	$\lambda$	$\sigma$	$\gamma$	$\varepsilon$	$\alpha$
Figure (3)	0.1	0.01	0.01	0.01	0.001	0.05	0.2	0.4	0.1
Figure (4)	0.1	0.01	0.01	0.01	0.01	0.05	0.2	0.4	0.1

**Table 2:** Table of parameter values used in simulations.

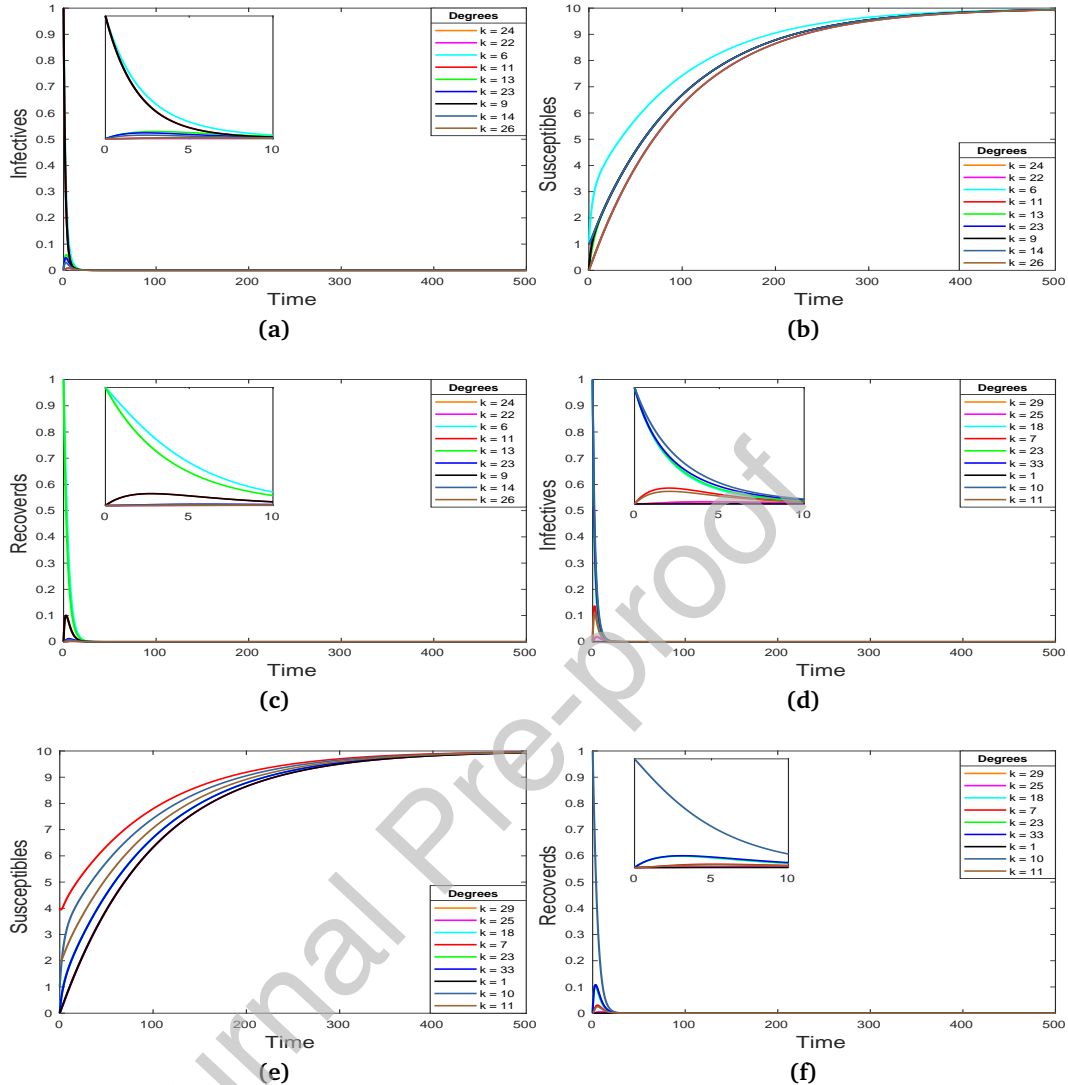


**Figure 3:** Figures (3a),(3b) and (3c) were obtained with the initial condition  $G_1$ . Whereas (3d),(3e) and (3f) were obtained starting from  $G_2$ .

In Figure 7 (d), the value  $\langle k^2 \rangle$  is represented in terms of consecutive sizes  $n = 100 \dots 800$ . One can remark that even for small number of connections  $m$  added in the process of growth of the BA model, the value of  $\langle k^2 \rangle$  quickly diverges. Whereas, as we remark in Figure 7 the numerical value of  $\langle k \rangle$  given by

$$\langle k \rangle_{num} = \sum_{i=1}^n i P_i$$

remains stable and is consistent with its theoretical value

$$\langle k \rangle_{th} = \sum_{i=1}^n i P_i^{th}, \quad (57)$$

where  $P_i^{th} = \frac{2m^2}{i^3}$ . The error  $\| < k >_{th} - < k >_{num} \|$  presented in Figure 7 becomes smaller as  $n$  goes to infinity. Therefore, we have

$$\lim_{n \rightarrow \infty} \mathcal{R}_0 = \lim_{n \rightarrow \infty} \frac{< k^2 >}{< k >} = \infty.$$

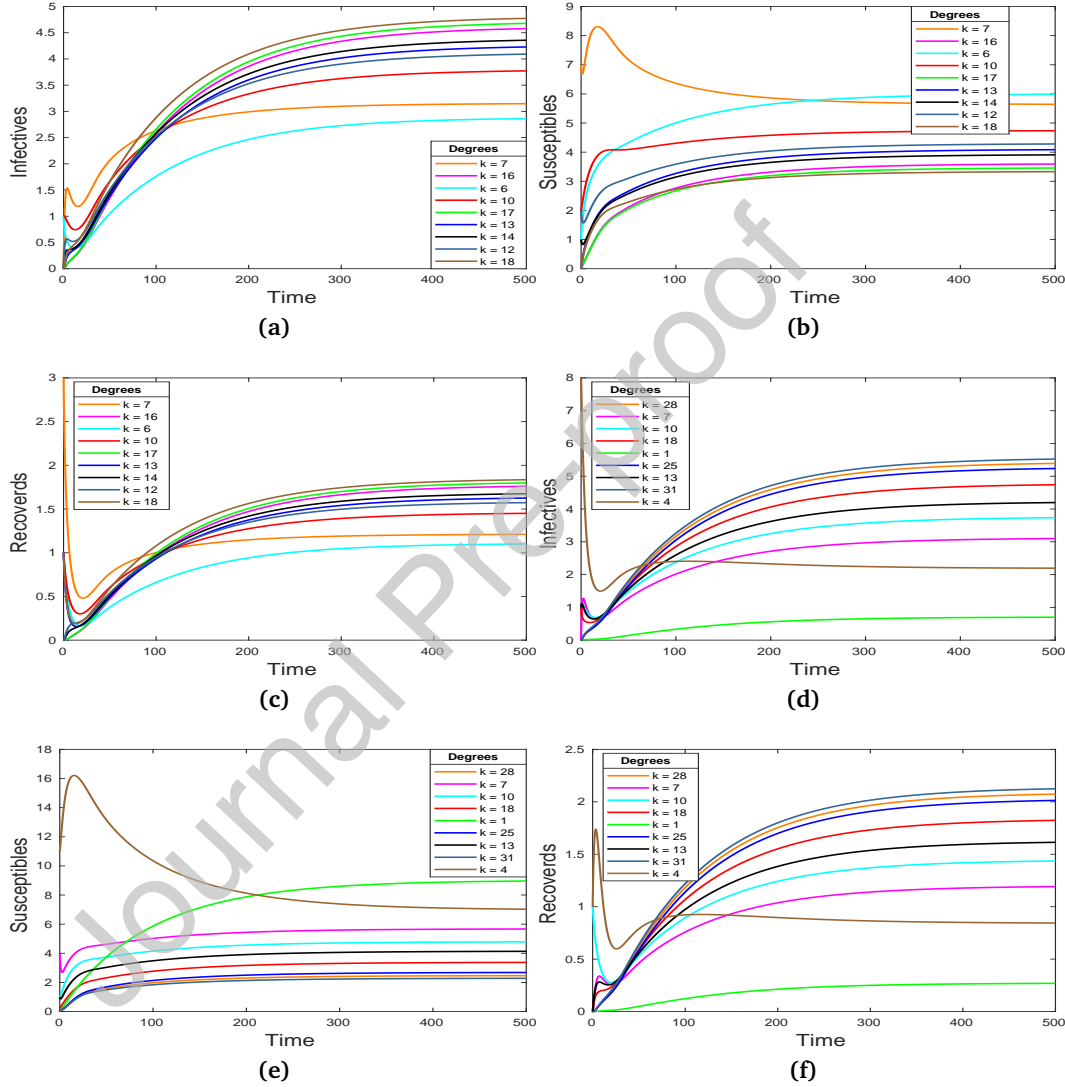


**Figure 4:** Simulations of the time series of  $S_k$ ,  $I_k$  and  $R_k$ . The figures (a),(b),(c) start from the initial condition represented by the graph  $G_1$ . Whereas, the figures (d),(e),(f) start from an initial population host depicted by  $G_2$ .

Thereby, in very large scale-free networks, this may justify the absence of the epidemic threshold as pointed out in [4, 35], and the disease always persists no matter how small is the infection rate  $\beta$ . Still, in "small" networks,  $\mathcal{R}_0$  is a key quantity that determines the behaviour of system (3). So, it is worthy to study how  $\mathcal{R}_0$  is sensitive to system's parameters. For this end, one can use Latin Hypercube Sampling/Partial Rank Correlation Coefficient (LHS/PRCC)

algorithm to study parameters sensitivity of  $\mathcal{R}_0$ . It is an efficient tool often employed in uncertainty analysis to explore the entire parameter space of a model with a minimum number of computer simulations. It involves the combination of two statistical techniques, Latin Hypercube Sampling (LHS), which was first introduced by McKay et al. in 1979 [28] and further developed by Iman et al. [17], and Partial Rank Correlation Coefficient (PRCC) analysis. The goal of LHS/PRCC sensitivity analysis is to identify key parameters whose uncertainties contribute to prediction imprecision and to rank these parameters by their importance in contributing to this imprecision [13]. Suppose we decide to do  $s$  model simulations (or runs) for our analysis. Also suppose there are  $U$  uncertain parameters,  $p_i$  with  $1 \leq i \leq U$ . Then the parameter space for the uncertain parameters would be defined by  $U$  dimensions. The choice of  $s$  is not arbitrary. If  $s$  is the number of simulations, the following inequality  $s > \frac{4}{3}U$  has to be satisfied. In our sensitivity analysis, we performed  $s = 1000$  runs, which is largely sufficient. In model (3), 11 parameters determine the value of  $\mathcal{R}_0$ . Namely,  $\langle k \rangle$ ,  $\langle k^2 \rangle$ ,  $\beta$ ,  $\mu$ ,  $\mu_1$ ,  $\mu_2$ ,  $\mu_3$ ,  $\alpha$ ,  $\gamma$ ,  $\sigma$  and  $\varepsilon$ . We consider two situations of sensitivity analysis to  $\mathcal{R}_0$ . In the first one, all the parameter values are fixed except  $\varepsilon$  and  $\sigma$ . The sampling was automatically generated for  $\varepsilon$  and  $\sigma$  using the function *lhsdesign\_modified* [31] by simply specifying the range of values.

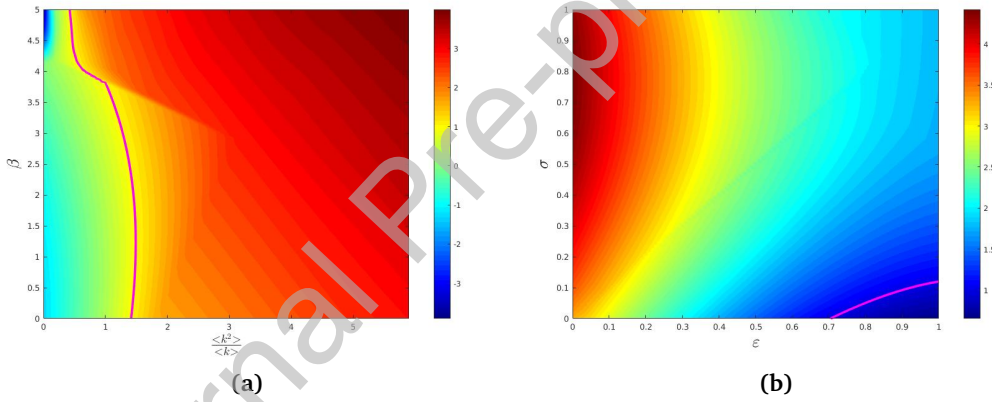


**Figure 5:** The basic reproduction number of system (3)  $\mathcal{R}_0$  is shown (a) when  $\beta$  is increased from 0 to 2 and  $\langle k \rangle$  is varied from 1 to 12 if  $\sigma = 0.3$ ,  $\varepsilon = 0.5$ ; (b) when  $\varepsilon$  is increased from 0 to 1 and  $\beta$  is varied from 0 to 1 if  $\langle k \rangle = 13.15$ ,  $\beta = 1.1$ . The solid pink line shows the contour line  $\mathcal{R}_0 = 1$ .

For the second case, we fixed all parameters except the infection rate  $\beta$  and the ratio  $\frac{\langle k^2 \rangle}{\langle k \rangle}$  which can be sampled by applying LHS on network's size  $n$ . Figure 5 (a) shows the relations of the reproduction number  $\mathcal{R}_0$  with the infection rate  $\beta$  and  $\frac{\langle k^2 \rangle}{\langle k \rangle}$ . One can affirm that the ratio  $\frac{\langle k^2 \rangle}{\langle k \rangle}$  linked to the scale-free network topology is very important and affects the value of the basic reproduction number  $\mathcal{R}_0$ . Even with a small infection rate  $\beta$  the disease can spread easily if its connectivity/mean degree ratio is high. Also, from Figure 5 (b), we can clearly see the effect of cure on the control of disease spread. If  $\varepsilon$  is greater the value of  $\mathcal{R}_0$  decreases, whereas if  $\sigma$  increases then  $\mathcal{R}_0$  increases also. To further investigate the sensitivity of  $\mathcal{R}_0$  to model's parameters, especially the most impacting parameter, elasticity is a powerful tool to help us in extracting this information. Using the definition of elasticity

$$E_{p_i} = \frac{p_i}{\mathcal{R}_0} \frac{\partial \mathcal{R}_0}{\partial p_i},$$

the elasticity of  $\mathcal{R}_0$  to the parameters,  $\beta$ ,  $\sigma$ ,  $\varepsilon$  and  $\alpha$  is shown in Figure 6. One can remark that  $\mathcal{R}_0$  is most elastic to  $p_3 = \varepsilon$ , as indicated by Figure 6. Because the elasticity of  $\mathcal{R}_0$  to  $\varepsilon$  is negative, a decrease in  $\varepsilon$  will result in an increase in  $\mathcal{R}_0$ . So, one can deduce that if the desired result is to reduce  $\mathcal{R}_0$ , then the most effective strategy must be to increase  $\varepsilon$ .

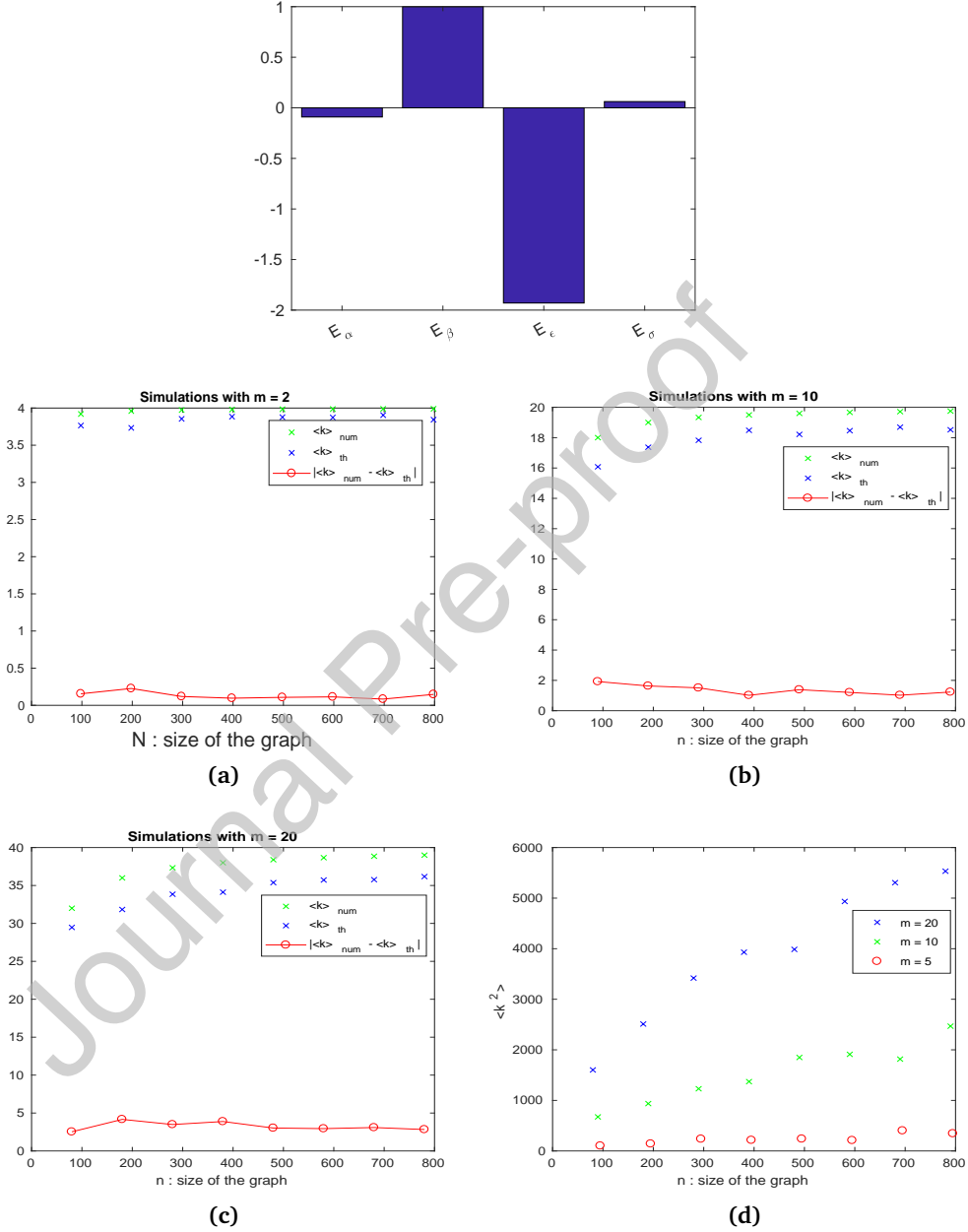


**Figure 7:** In graphs (a),(b) and (c) we show simultaneously the values of the theoretical and numerical values of  $\langle k \rangle$  and the difference between them for different sizes  $n$  and connections  $m$ . Graph (d) represents the relation between  $n$  the size of the network and the connectivity  $\langle k^2 \rangle$ .

## References

- [1] A. Barabási, R. Albert, Emergence of scaling in random networks, *science* **1999**, *286*, 509–512.
- [2] A. Barabasi, Z. N. Oltvai, Network biology: understanding the cell's functional organization, *Nature reviews genetics* **2004**, *5*, 101.
- [3] E. Beretta, Y. Takeuchi, Global stability of an SIR epidemic model with time delays, *Journal of mathematical biology* **1995**, *33*, 250–260.
- [4] S. Boccaletti, V. Latora, Y. Moreno, M. Chavez, D.-U. Hwang, Complex networks: Structure and dynamics, *Physics reports* **2006**, *424*, 175–308.
- [5] B. Bollobás, O. Riordan, J. Spencer, G. Tusnády, The degree sequence of a scale-free random graph process, *Random Structures & Algorithms* **2001**, *18*, 279–290.
- [6] B. Bollobás, F. R. K. Chung, The diameter of a cycle plus a random matching, *SIAM Journal on discrete mathematics* **1988**, *1*, 328–333.
- [7] S. Bornholdt, H. G. Schuster, Handbook of graphs and networks: from the genome to the internet, John Wiley & Sons, **2006**.
- [8] J. Cao, Y. Wang, A. Alofi, A. Al-Mazrooei, A. Elaiw, Global stability of an epidemic model with carrier state in heterogeneous networks, *IMA Journal of Applied Mathematics* **2014**, *80*, 1025–1048.
- [9] A. d'Onofrio, A note on the global behaviour of the network-based SIS epidemic model, *Nonlinear Analysis: Real World Applications* **2008**, *9*, 1567–1572.
- [10] P. van den Driessche, J. Watmough, A simple SIS epidemic model with a backward bifurcation, *Journal of Mathematical Biology* **2000**, *40*, 525–540.
- [11] P. Erdős, A. Rényi, On the existence of a factor of degree one of a connected random graph, *Acta Mathematica Hungarica* **1966**, *17*, 359–368.
- [12] P. Erds, A. Rényi, On the evolution of random graphs, *Publ. Math. Inst. Hungar. Acad. Sci* **1960**, *5*, 17–61.
- [13] B. Gomero, Latin Hypercube Sampling and Partial Rank Correlation Coefficient analysis applied to an optimal control problem, **2012**.
- [14] H. Gonzalez-Diaz, L. Perez-Montoto, A. Duardo-Sanchez, E. Paniagua, S. Vazquez-Prieto, R. Vilas, M. Dea-Ayuela, F. Bolas-Fernandez, C. Munteanu, J. Dorado, et al., Generalized lattice graphs for 2D-visualization of biological information, *Journal of theoretical biology* **2009**, *261*, 136–147.
- [15] J. A. Hadley, N. V. Kraguljac, D. M. White, L. Ver Hoef, J. Tabora, A. C. Lahti, Change in brain network topology as a function of treatment response in schizophrenia: a longitudinal resting-state fMRI study using graph theory, *npj Schizophrenia* **2016**, *2*, 16014.
- [16] H. W. Hethcote, P. Van den Driessche, An SIS epidemic model with variable population size and a delay, *Journal of Mathematical Biology* **1995**, *34*, 177–194.
- [17] R. L. Iman, W. J. Conover, The use of the rank transform in regression, *Technometrics* **1979**, *21*, 499–509.

- [18] H. Kim, Z. Toroczkai, P. L. Erdős, I. Miklós, L. A. Székely, Degree-based graph construction, *Journal of Physics A: Mathematical and Theoretical* **2009**, *42*, 392001.
- [19] A. Korobeinikov, Lyapunov Functions and Global Stability for SIR and SIRS Epidemiological Models with Non-Linear Transmission, *Bulletin of Mathematical Biology* **2006**, *68*, 615–626.
- [20] A. Lahrouz, H. El Mahjour, A. Settati, A. Bernoussi, Dynamics and optimal control of a non-linear epidemic model with relapse and cure, *Physica A: Statistical Mechanics and its Applications* **2018**, *496*, 299–317.
- [21] C. Li, C. Tsai, S. Yang, Analysis of epidemic spreading of an SIRS model in complex heterogeneous networks, *Communications in Nonlinear Science and Numerical Simulation* **2014**, *19*, 1042–1054.
- [22] L. Li, Monthly periodic outbreak of hemorrhagic fever with renal syndrome in China, *Journal of Biological Systems* **2016**, *24*, 519–533.
- [23] L. Li, J. Zhang, C. Liu, H. Zhang, Y. Wang, Z. Wang, Analysis of transmission dynamics for Zika virus on networks, *Applied Mathematics and Computation* **2019**, *347*, 566–577.
- [24] J. Liu, T. Zhang, Epidemic spreading of an SEIRS model in scale-free networks, *Communications in Nonlinear Science and Numerical Simulation* **2011**, *16*, 3375–3384.
- [25] L. Liu, J. Wang, X. Liu, Global stability of an SEIR epidemic model with age-dependent latency and relapse, *Nonlinear Analysis: real world applications* **2015**, *24*, 18–35.
- [26] N. Masuda, N. Konno, Multi-state epidemic processes on complex networks, *Journal of Theoretical Biology* **2006**, *243*, 64–75.
- [27] C. C. McCluskey, Delay versus age-of-infection–global stability, *Applied Mathematics and Computation* **2010**, *217*, 3046–3049.
- [28] M. D. McKay, R. J. Beckman, W. J. Conover, Comparison of three methods for selecting values of input variables in the analysis of output from a computer code, *Technometrics* **1979**, *21*, 239–245.
- [29] S. Moghadas, A. Gumel, A mathematical study of a model for childhood diseases with non-permanent immunity, *Journal of computational and applied Mathematics* **2003**, *157*, 347–363.
- [30] Y. Muroya, H. Li, T. Kuniya, Complete global analysis of an SIRS epidemic model with graded cure and incomplete recovery rates, *Journal of Mathematical Analysis and Applications* **2014**, *410*, 719–732.
- [31] K. Nassim, Latin Hypercube Sampling Matlab Function, <https://www.mathworks.com/matlabcentral/fileexchange/45793-latin-hypercube>, A Matlab Free Resource.
- [32] M. E. Newman, D. J. Watts, S. H. Strogatz, Random graph models of social networks, *Proceedings of the National Academy of Sciences* **2002**, *99*, 2566–2572.
- [33] S. Ni, W. Weng, S. Shen, W. Fan, Epidemic outbreaks in growing scale-free networks with local structure, *Physica A: Statistical Mechanics and its Applications* **2008**, *387*, 5295–5302.

- [34] W. H. Organization, Immunization, Vaccines and Biologicals, <http://www.who.int/immunization/diseases/en/>, Appeared in an answer in Stack Exchange forum of physics.
- [35] R. Pastor-Satorras, A. Vespignani, Epidemic spreading in scale-free networks, *Physical review letters* **2001**, 86, 3200.
- [36] R. Pastor-Satorras, A. Vespignani, Epidemic dynamics in finite size scale-free networks, *Physical Review E* **2002**, 65, 035108.
- [37] L. Perko, Differential equations and dynamical systems, Vol. 7, Springer Science & Business Media, **2013**.
- [38] M. Tomassini, Introduction to graphs and networks, *Information Systems Department HEC University of Lausanne Switzerland* **2010**.
- [39] Unknown, Network topology, <https://i.stack.imgur.com/6IqoM.png>.
- [40] P. Van den Driessche, X. Zou, Modeling relapse in infectious diseases, *Mathematical biosciences* **2007**, 207, 89–103.
- [41] P. Van den Driessche, J. Watmough, Reproduction numbers and sub-threshold endemic equilibria for compartmental models of disease transmission, *Mathematical biosciences* **2002**, 180, 29–48.
- [42] C. Vargas-De-León, On the global stability of infectious diseases models with relapse, *Abstraction and Application Magazine* **2014**, 9.
- [43] L. Wang, G. Dai, Global stability of virus spreading in complex heterogeneous networks, *SIAM Journal on Applied Mathematics* **2008**, 68, 1495–1502.
- [44] Y. Wang, J. Cao, M. Li, L. Li, Global behavior of a two-stage contact process on complex networks, *Journal of the Franklin Institute* **2019**, 356, 3571–3589.
- [45] Y. Wang, J. Cao, Global dynamics of a network epidemic model for waterborne diseases spread, *Applied Mathematics and Computation* **2014**, 237, 474–488.
- [46] Y. Wang, J. Cao, A. Alsaedi, T. Hayat, The spreading dynamics of sexually transmitted diseases with birth and death on heterogeneous networks, *Journal of Statistical Mechanics: Theory and Experiment* **2017**, 2017, 023502.
- [47] Y. Wang, J. Ma, J. Cao, L. Li, Edge-based epidemic spreading in degree-correlated complex networks, *Journal of theoretical biology* **2018**, 454, 164–181.
- [48] D. J. Watts, Small worlds: the dynamics of networks between order and randomness, Vol. 9, Princeton university press, **2004**.
- [49] D. J. Watts, Networks, Dynamics, and the Small-World Phenomenon, *American Journal of Sociology* **1999**, 105, 493–527.
- [50] D. J. Watts, S. H. Strogatz, Collective dynamics of ‘small-world’networks, *nature* **1998**, 393, 440.
- [51] L. Weinstein, Empirical Study of Graph Properties with Particular Interest Towards Random Graphs, Institutional Scholarship TriCollege Libraries, **2005**.
- [52] E. W. Weisstein, Lattice Graph, <http://mathworld.wolfram.com/LatticeGraph.html>, A Wolfram Web Resource.

- [53] R. Xu, Global dynamics of a delayed epidemic model with latency and relapse, *Nonlinear Anal. Model. Control* **2013**, *18*, 250–263.
- [54] J. Yang, L. Wang, X. Li, F. Zhang, Global dynamical analysis of a heroin epidemic model on complex networks, *JOURNAL OF APPLIED ANALYSIS AND COMPUTATION* **2016**, *6*, 429–442.
- [55] H. Zhang, X. Fu, Spreading of epidemics on scale-free networks with nonlinear infectivity, *Nonlinear Analysis Theory Methods and Applications* **2009**, *70*, 3273–3278.
- [56] G. Zhu, X. Fu, G. Chen, Spreading dynamics and global stability of a generalized epidemic model on complex heterogeneous networks, *Applied Mathematical Modelling* **2012**, *36*, 5808–5817.